

Microsegregation induced microstructures in intermetallic Ti-46Al-8Nb alloy

J. Zollinger^{1,2*}, Z. Gabalcová³, D. Daloz¹, J. Lapin³, H. Combeau¹

¹Laboratoire de Science et Génie des Matériaux et de Métallurgie, Ecole Nationale Supérieure des Mines de Nancy, Parc de Saurupt, F-54042 Nancy, Cedex, France

²ACCESS e.V., Intzestr. 5, 52072 Aachen, Germany

³Institute of Materials and Machine Mechanics, Slovak Academy of Sciences, Račianska 75, 831 02 Bratislava, Slovak Republic

Received 14 July 2008, received in revised form 11 September 2008, accepted 11 September 2008

Abstract

The present work highlights the build up of the microsegregation coming from both solidification and high temperature solid state transformation in Ti-46Al-8Nb (at.%) alloy prepared by quench during directional solidification (QDS) experiments. Microstructure analysis of the QDS samples associated with quantitative chemical analysis were performed and compared to as-cast structures and heterogeneities. It is found that the microsegregation formed during solidification favours the $\beta \rightarrow \alpha$ solid state transformation at higher temperatures and thus intensifies the solid state segregation.

Key words: titanium aluminides, TiAl, solidification, phase transformations, microstructure

1. Introduction

With low density, high specific strength, high Young's modulus and oxidation resistance, TiAl-based alloys have attracted attention as a good alternative to nickel-based superalloys for high-temperature structural applications in the aerospace and automotive industries [1, 2]. The best compromise among various properties required for high temperature structural application is achieved with fine grained material containing $\alpha_2(\text{Ti}_3\text{Al})/\gamma(\text{TiAl})$ lamellar structure, which creep or oxidation resistance can be further improved with alloying elements such as Nb, Ta, Si, Zr or W [3–8]. Grain refinement is achieved by appropriate heat treatments and it is improved with solidifying through the β phase (Ti based solid solution with cubic crystal structure) [9]. However, the use of β -stabiliser elements such as Nb leads to the stabilisation of the β phase at lower temperatures in the form of ordered B2 or β_0 phase. Various structures and types of segregation observed in as-cast high niobium containing TiAl-based alloys have been reported by several au-

thors [10–13]. Chen et al. [13] observed three types of microsegregation in Ti-45Al-(8-9)Nb-(W,B,Y) (at.%) alloy: (i) interdendritic γ phase inherited from solidification (S-segregation), (ii) intradendritic niobium-rich areas coming from the $\beta \rightarrow \alpha$ (Ti based solid solution with hexagonal crystal structure) solid state transformation (β -segregation) and (iii) intralamellar β phase formed during the $\alpha \rightarrow \alpha + \gamma + \beta$ transformation (α -segregation). According to these authors [13], hot isostatic pressing (HIP) treatment does not allow reducing volume fraction of the β phase. Therefore, high cooling rates in the temperature range of the $\beta \rightarrow \alpha$ transformation were proposed to reduce Nb diffusion and thus to limit the amount of the β phase. A recent study by Zollinger et al. [14] has shown that only S-segregation and β -segregation occur in as-cast Ti-46Al-8Nb (at.%) alloy. The as-cast microstructure of this alloy is composed of α_2/γ lamellar structure, B2 phase, and monolithic γ phase formed in the interdendritic regions [6]. For the clarity, the B2 phase but also the chemical heterogeneities formed during the $\beta \rightarrow \alpha$ transformation observed at

*Corresponding author: tel.: +49-(0)-241-80-98018; fax: +49-(0)-241-38578; e-mail address: julien.zollinger@access.rwth-aachen.de

room temperature will be called β in this paper, as only high temperature phase transformations are considered.

The aim of the present work is to study the microstructure and microsegregations inherited from solidification and high temperature solid phase transformations in an intermetallic Ti-46Al-8Nb (at.%) alloy prepared by quench during directional solidification (QDS) experiments described elsewhere [6]. The origin and evolution of microsegregation are analysed and discussed, based on both thermodynamic equilibria and kinetic considerations. During directional solidification, the growth conditions are well controlled and the alloy solidifies by pulling the sample at a defined rate into a known temperature gradient. The quench allows observing not only the microstructures and chemical heterogeneities formed during solidification but their evolution in the solid state at room temperature as well. More, the quench permits to observe the effect of high cooling rate on microstructure formation.

2. Experimental procedure

QDS experiments were performed in dense Y_2O_3 crucibles (purity of 99.5 %) with a diameter of 8/12 mm (inside/outside diameter) and length of 130 mm using a Bridgman type apparatus described elsewhere [15]. The experiments were carried out at constant growth rates V_p ranging from 5.56×10^{-6} to $118 \times 10^{-6} \text{ m s}^{-1}$ and at constant temperature gradients in liquid at the solid-liquid interface G_L ranging from 4000 to 8000 K m^{-1} . Such growth conditions resulted in cooling rates ranging from 1.9×10^{-2} to $9.4 \times 10^{-1} \text{ K s}^{-1}$. The samples were quenched by a rapid displacement of the mould into the water-cooled crystalliser after a length of 50 mm has been solidified. The cooling rate of the quench is of the order of 50 K s^{-1} .

Microstructure analysis was performed by scanning electron microscopy in backscattered electrons mode (BSE). Samples were prepared using standard metallographic techniques (grinding and polishing). Samples for BSE observations were polished with colloidal silica with 30 % H_2O_2 . Preparation of samples for energy dispersive spectrometry (EDS) analysis and electron probe microanalysis (EPMA) wavelength dispersive spectrometry (WDS) followed the procedure described elsewhere [16]. EPMA was calibrated using standards of pure Ti (99.99 %), pure Al (99.999 %) and Nb (99.99 %). Quantitative metallographic analysis concerning volume fraction of co-existing phases was performed by a computerised image analyser. Phases were identified with X-ray diffraction (XRD) using a SIEMENS D500 diffractometer.

3. Results

Figure 1a shows the typical macrograph of the QDS samples. One can distinguish three different zones from the top to the bottom of the quenched sample marked in the figure: (i) the liquid zone (1), (ii) the mushy zone (2) and (iii) the directionally solidified solid zone (3). The mushy zone (2) shows a dendritic pattern with primary dendrite arms growing parallel to the withdrawal direction. The contrast of the dendritic pattern almost disappears once reaching the fully solidified part (zone 3). Representative BSE images of characteristic microstructures of zones 2 and 3 are depicted in Figs. 1b, 1c and 1d and the selected positions for these pictures are marked in Fig. 1a. Figure 1b shows the typical microstructure observed in the mushy zone, i.e. the part of the sample quenched from the β + liquid (L) domain. It can be distinguished in the figure a grey contrast covering all over with a white network, except in the darker areas that correspond to the former interdendritic liquid. EDS analysis performed on the white network shows higher Nb and lower aluminium content than in the surrounding areas. Assuming XRD results that have shown some amount of the β phase in the microstructure, the white network corresponds to the β phase that has been retained due to the incompleteness of the β to α phase transformation. The grey areas correspond then to the α phase. Both grey and white contrasts are covered with the $\alpha_2(\text{Ti}_3\text{Al})/\gamma(\text{TiAl})$ lamellar structure (not visible at such magnification). The black regions consist of quenched liquid that is enriched in aluminium and depleted in niobium. While partly formed during the quench and partly formed during directional solidification, one may note that the microstructure is similar to that described for example by Zollinger et al. [14] in as-cast and Gabalcová and Lapin [6] in directionally solidified Ti-46Al-8Nb (at.%) alloy, i.e. it is the typical microstructure formed at relatively high cooling rate (10 K s^{-1}). Just below the mushy zone at about 1773 K (Fig. 1c), the microstructure is similar to that observed in the quenched mushy zone. It is composed of α_2 laths with some retained β phase under the appearance of a very fine basket weave microstructure. In this part of the quenched sample, the basket weave microstructure covers all the area including the former interdendritic zone. From this observation it can be concluded that this area was quenched from the single β phase region. At lower temperature of 1753 K, the microstructure is again similar to that described above and is composed of α phase and residual β phase (Fig. 1d). However, in this case, the phase distribution leads to a coarser basket weave microstructure indicating that the $\beta \rightarrow \alpha$ transformation has occurred at lower cooling rates, i.e. during the directional solidification and thus corresponds to an “equilibrium” transformation. The distance $d_{\beta/\beta}$

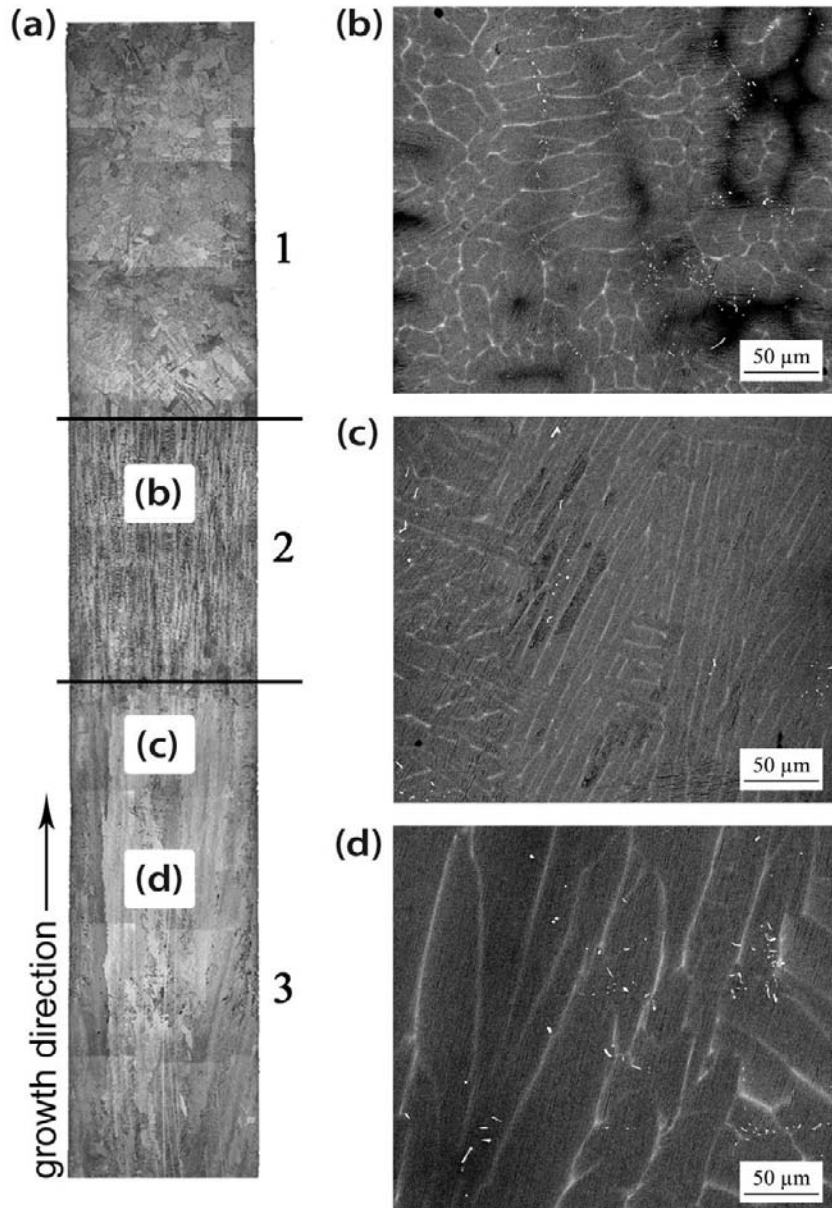


Fig. 1. (a) Macrograph of the 8 mm diameter QDS sample solidified at $V_p = 118 \times 10^{-6} \text{ m s}^{-1}$ and $G_L = 4000 \text{ K m}^{-1}$: 1 – quenched liquid (L), 2 – mushy zone, 3 – directionally solidified solid; (b) BSE micrograph showing microstructure in the mushy zone quenched from 1822 K; (c) BSE micrograph showing microstructure in the single β phase domain quenched from 1773 K and (d) BSE micrograph showing microstructure in the directionally solidified solid quenched from 1753 K.

measured between residual β phase with the intercept method evolves from $d_{\beta/\beta} = 16.2 \mu\text{m}$ in the mushy zone, to $d_{\beta/\beta} = 7.3 \mu\text{m}$ at 1773 K and finally to $d_{\beta/\beta} = 40 \mu\text{m}$ at 1753 K.

The chemical analysis was performed on the samples solidified at different growth conditions by means of EPMA. However, this work is focused only on the chemical analysis of the sample prepared at $V_p = 118 \times 10^{-6} \text{ m s}^{-1}$ and $G_L = 4000 \text{ K m}^{-1}$ (Fig. 1), which can be considered as the typical example of all studied QDS samples. The average composition of this sample resulting from the statistical

measurements is Ti-45.9Al-8.6Nb (at.%). Table 1 gives the average chemical composition measured along the samples at different locations characterised by their temperature before the quench. It is clear that there is no shift in the chemical composition of the alloy along the withdrawal direction.

Figure 2 shows the details of WDS profiles measured for niobium. Several observations can be made from this figure. In the mushy zone at 1834 K (Fig. 2a) and 1822 K (Fig. 2b), the segregation amplitude is important. It can be analysed in two parts depending on its origin. The largest segregation amplitude

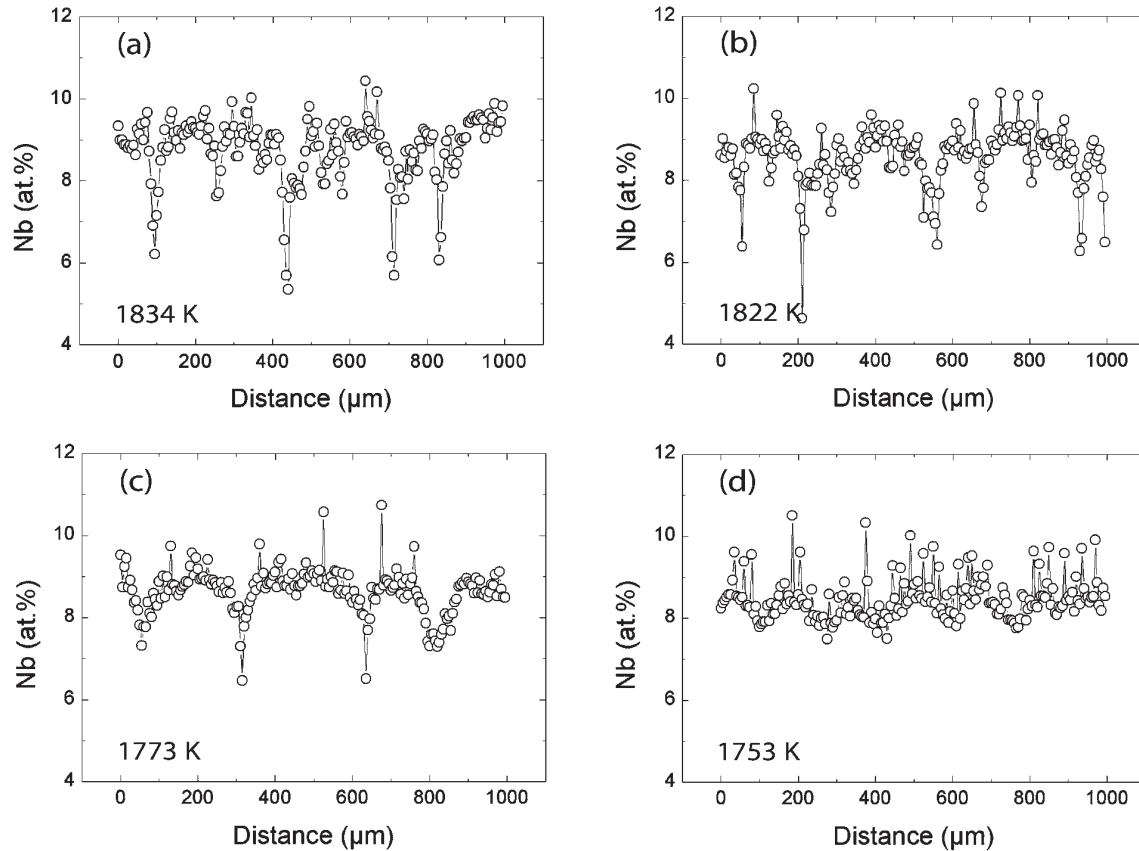


Fig. 2. WDS profiles measured for niobium in the QDS sample prepared at $V_p = 118 \times 10^{-6} \text{ m s}^{-1}$ and $G_L = 4000 \text{ K m}^{-1}$: (a) 1834 K, (b) 1822 K, (c) 1773 K and (d) 1753 K.

Table 1. Average chemical composition measured along the samples at different locations characterised by their temperature before the quench

Temperature (K)	Al (at.%)	Nb (at.%)
1753	45.9 ± 0.8	8.6 ± 0.6
1773	45.9 ± 1.3	8.5 ± 0.7
1822	45.8 ± 1.3	8.7 ± 0.8
1834	45.9 ± 1.4	8.5 ± 0.9

corresponds to the lowest niobium values. Those values, typically lower than the 8.3 at.% of the average composition, correspond to the interdendritic regions. This type of segregation is inherited from the solidification. Another contribution to the segregation amplitude can be found in niobium rich regions, thus in the intradendritic regions, and can be attributed to the residual β phase identified previously. This type of segregation is inherited from the β to α solid state transformation. At 1773 K (Fig. 2c), both inter- and intradendritic segregations decrease and at 1753 K (Fig. 2d), the interdendritic segregation has almost disappeared. Instead, a new segregation appears corresponding to the “equilibrium” $\beta \rightarrow \alpha$ transforma-

tion, where the residual β phase corresponds to high Nb values in Fig. 2. Similar profiles have been observed in all analysed QDS samples. Hence, it is unambiguous that the segregation amplitude decreases sharply once the solid state is reached.

4. Discussion

The first relevant result of this study is that no traces of a peritectic transformation, as described for example by Fredriksson and Nylén [17], have been observed in the QDS samples neither in the microstructures nor indicated by the chemical analysis. When looking at existing phase diagrams (see for instance the isopleth Ti-Al-8Nb section reported recently by Chen et al. [18]), the proximity of the peritectic valley from the nominal composition of the studied alloy makes such a peritectic transformation expectable. Thermodynamic calculations performed with the Scheil approximation and the database dedicated to the Ti-Al-Nb system by Witusiewicz et al. [19] clearly predict the formation of a significant amount of peritectic α phase during solidification. The fact that no peritectic transformation was observed in the studied alloy can thus be attributed to the selected solidifica-

tion processing parameters that involve growth close to the thermodynamic equilibrium.

The second relevant result concerns the evolution and the morphology of the residual β phase. All microstructures shown above revealed the presence of α colonies with some retained β phase between the α laths, even in the zones quenched from the β or $L + \beta$ domains. This can be attributed to both microsegregation and kinetic effects. It was shown that:

- once the solidification is complete, the alloy homogenises quickly, i.e. we can consider that the composition in this area is rather homogeneous,
- in the mushy zone, the alloy is heterogeneous at the dendrite scale with higher Al content (resp. lower Nb content) at the secondary arms tips.

From these observations, two main reasons explaining the difference of the observed morphology of the residual β phase can be formulated. The first one is that due to microsegregation the regions close to the solid-liquid interface (Al-rich and Nb-poor) in the mushy zone should start the $\beta \rightarrow \alpha$ transformation at higher temperature. In order to check this point, we performed thermodynamic calculations using the Ti-Al-Nb database [18] for two different compositions: (i) the nominal chemical composition of the studied alloy and the measured composition corresponding to the secondary dendrite arms. The results of these calculations are shown in Fig. 3 in the form of a dependence of the volume fraction of the α phase on the temperature. From this figure it is clear that the calculated $\beta \rightarrow \alpha$ transformation starts at a temperature of 1791 K for composition of Ti-48Al-6Nb (at.%) corresponding to the segregated areas measured in SDA and is by 25 K higher than that of 1766 K calculated for the alloy with the nominal composition of Ti-45.9Al-8.9Nb (at.%). In addition, the $\beta \rightarrow \alpha$ transformation interval of 15 K is significantly lower for the segregated areas than that of 70 K for the alloy with the nominal composition. The second point is that the mushy zone is quenched from a temperature of about 50 K higher than the single β domain. It means that the difference of the diffusion length between these two areas will be, for example for aluminium $\sqrt{D_{\text{Al}}^{\beta} \cdot t} \approx 7 \times 10^{-6}$ m taking diffusion coefficient of $D_{\text{Al}}^{\beta} \approx 5.5 \times 10^{-11}$ m² s⁻¹ extrapolated from the data reported by Mishin and Herzig [20] and assuming cooling time of $\Delta t = 1$ s for quenching at a cooling rate of about 50 K s⁻¹. The combination of these two phenomena seems to induce the observed difference in size and morphology of the residual β phase. The release of latent heat due to the solidification during the quench has not been considered here as a contribution to the observed different colony sizes. Indeed, 5 K below the liquidus temperature the solidified fraction is higher than 80 % and becomes higher than 90 % at 10 K below the liquidus. Hence, the latent heat released by the small fraction of re-

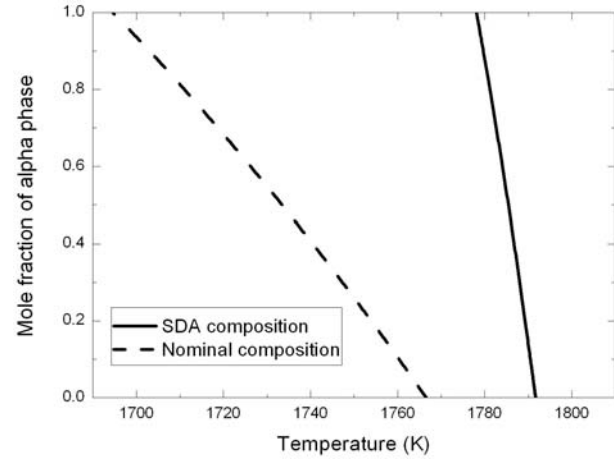


Fig. 3. Evolution of the mole fraction of α phase with temperature calculated with the Thermo-Calc[®] software and Ti-Al-Nb database [19] for the measured nominal chemical composition of Ti-45.9Al-8.9Nb (at.%) and for the composition of Ti-48Al-6Nb (at.%) resulting from the measurements in the secondary dendrite arms (SDA).

maining liquid during the quench was thus neglected in the discussion.

These results show that not only the cooling rate has an influence on the β -segregation formation but the microsegregation developed during solidification is also an important parameter. Chen et al. [13] applied fast cooling rate in the temperature range of $\beta \rightarrow \alpha$ transformation to reduce β -segregation. The use of a process with high cooling rate will have the consequence to increase the microsegregation as the solidification will tend to a Scheil-type solidification (limited diffusion in the solid phase during freezing). From the observations made above, it is clear that increasing intradendritic microsegregation will favour α growth at higher temperature, leading to the microstructures observed in the mushy zone of the samples which are comparable to those obtained previously in cold crucible ingots [14].

5. Conclusions

The investigation of microstructure formation in Ti-46Al-8Nb (at.%) alloy during the solidification and the subsequent $\beta \rightarrow \alpha$ solid state transformation suggests the following conclusions:

1. No peritectic transformation occurs in this alloy that fully solidifies within the β phase. The $\beta \rightarrow \alpha$ solid state transformation occurs even in parts of the QDS samples quenched from the β or $L + \beta$ domains, leading to microstructures composed of α phase and retained β phase.
2. The heterogeneities built-up during solidification

allow the $\beta \rightarrow \alpha$ transformation to start at higher temperatures. At equivalent cooling rate, and compared to rather homogeneous areas of the samples quenched from the single β phase domain, this α stabilising effect due to microsegregation leads to coarser microstructures and intensifies inherent solid state segregations.

Acknowledgements

This work was financially supported by EU Integrated Project IMPRESS “Intermetallic Materials Processing in Relation to Earth and Space Solidification” under the contract No. NMP3-CT-2004-500635. J. Zollinger would like to thank U. Hecht for her constructive comments. One of the authors (J. Lapin) would like to thank also the Slovak Research and Development Agency under the contract APVV-0009-07 for the financial support.

References

- [1] KIM, Y. W.: JOM, 46, 1994, p. 30.
- [2] AUSTIN, C. M.—KELLY, T. J.: In: Gamma Titanium Aluminides. Eds.: Kim, Y. W., Wagner, R., Yamaguchi, M. Warrendale, TMS 1995, p. 21.
- [3] YOSHIHARA, M.—MIURA, K.: Intermetallics, 3, 1995, p. 357.
- [4] LAPIN, J.—GABALCOVÁ, Z.—BAJANA, O.—DALOZ, D.: Kovove Mater., 44, 2006, p. 297.
- [5] LAPIN, J.: Kovove Mater., 44, 2006, p. 57.
- [6] GABALCOVÁ, Z.—LAPIN, J.: Kovove Mater., 45, 2007, p. 177.
- [7] LAPIN, J.—PELACHOVÁ, T.—DOMÁNKOVÁ, M.—DALOZ, D.—NAZMY, M.: Kovove Mater., 45, 2007, p. 121.
- [8] LAPIN, J.—GABALCOVÁ, Z.: Kovove Mater., 46, 2008, p. 185.
- [9] JIN, Y.—WANG, J. N.—YANG, J.—WANG, Y.: Scripta Mater., 51, 2004, p. 113.
- [10] HUANG, Z. W.: Scripta Mater., 52, 2005, p. 1021.
- [11] XU, X. J.—LIN, J. P.—WANG, Y. L.—CHEN, G. L.: Journal of University of Science and Technology, Beijing, 12, 2005, p. 134.
- [12] XU, X. J.—LIN, J. P.—TENG, Z. K.—WANG, Y. L.—CHEN, G. L.: Mater. Lett., 369, 2006, p. 373.
- [13] CHEN, G. L.—XU, X. J.—TENG, Z. K.—WANG, Y. L.—LIN, J. P.: Intermetallics, 15, 2007, p. 625.
- [14] ZOLLINGER, J.—DALOZ, D.—LAPIN, J.—COMBEAU, H.: In: Proceedings of the 5th Decennial International Conference on Solidification Processing. Ed.: Jones, H. Sheffield, The University of Sheffield 2007, p. 282.
- [15] LAPIN, J.—ONDRŮŠ, L.—NAZMY, M.: Intermetallics, 10, 2002, p. 1019.
- [16] ZOLLINGER, J.—LAPIN, J.—DALOZ, D.—COMBEAU, H.: Intermetallics, 15, 2007, p. 1343.
- [17] FREDRIKSSON, H.—NYLÉN, G.: Metal Science, 16, 1982, p. 283.
- [18] CHEN, G.—ZHANG, W.—LIU, Z.—LI, S.—KIM, Y. W.: In: Gamma Titanium Aluminides. Eds.: Kim, Y. W., Dimiduk, D. M., Loretto, M. H. Warrendale, TMS 1999, p. 371.
- [19] WITUSIEWICZ, V. T.—BONDAR, A. A.—HECHT, U.—REX, S.—VELIKANOVA, T. Y.: J. Alloys Compd., 2008, doi: 10.1016/j.jallcom.2008.05.008.
- [20] MISHIN, Y.—HERZIG, C.: Acta Mater., 48, 2000, p. 589.